Environ Monit Assess (2011) 174:187–197
DOI 10.1007/s10661-010-1449-9

# Nanominerals and nanoparticles in feed coal and bottom ash: implications for human health effects

**Luis F. O. Silva · Kátia M. da Boit**

Received: 21 January 2010 / Accepted: 6 April 2010 / Published online: 27 April 2010


**Abstract** Environmental and human health risk assessments of nanoparticle effects from coal and bottom ash require thorough characterisation of nanoparticles and their aggregates. In this manuscript, we expand the study of human exposure to nanosized particles from coal combustion sources (typically <100 nm in size), characterising the complex micromineralogy of these airborne combustion-derived nanomaterials. Our study focuses on bottom ash generated in the Santa Catarina power station (Brazil) which uses coal enriched in ashes, many potential elements (e.g. Cr and Ni) and pyrite. Transmission electron microscope data reveal nanoscale C deposits juxtaposed with and overgrown by slightly larger aluminosilicate (Al–Si) glassy spheres, oxides, silicates, carbonated, phosphates and sulphates. Iron oxides (mainly hematite and magnetite) are the main bottom ash products of the oxidation of pyrite, sometimes via intermediate pyrrhotite formation. The presence of iron oxide nanocrystals mixed with silicate glass particles emphasises the complexity of coal and bottom ash micromineralogy. Given the potentially bioreactive nature of such transition metal-bearing materials, there is likely to be an increased health risk associated with their inhalation.

**Keywords** Coal · Bottom ash · Nanominerals · Human exposure

L. F. O. Silva (✉) · K. M. da Boit
Catarinense Institut of Environmental Research and Human Development, IPADHC,
Capivari de Baixo, Santa Catarina, Brazil
e-mail: felipeqma@yahoo.com.br

## Introduction

Human health impacts of combustion-derived nanomaterials (CDNs, <100 nm in size) released to the environment are gaining increasing worldwide interest, especially since exposure to CDNs has increased dramatically within the past century. Epidemiological studies have clearly indicated a relationship between increasing human morbidity and mortality, and progressive environmental air pollution caused by particles (e.g. Rastogi et al. 2009; Effros 2009; An et al. 2007; Liang-Che et al. 2006; Chen et al. 2004, 2005; Tatár et al. 2005; Suzuki et al. 2002). The greater surface areas of ultrafine CDNs compared with larger particles with the same chemical compositions make them more environmentally active with respect to biouptake and associated health risks (Gilmour et al. 2004; Oberdoerster et al. 2005; Xia et al. 2006). Coal combustion is a key issue in the study of CDNs, given the complex organic and inorganic chemistry of the materials involved; the abundance of coal resources throughout the world; and their

importance to the economies of major, rapidly developing countries such as China, India and Brazil. These findings suggest that the effect of feed coal emissions may be important not only on a local or regional scale but also nationally and internationally. The main drawback of coal-fired power plants in Brazil is the high production of ash. The coal used in Brazilian power plants is pulverised and burned inside a boiler, producing bottom ash (15–20 wt.% of the bulk solid combustion by-products produced), which falls inside the boiler (Depoi et al. 2008) and does not find at present time a commercial application; rather, it is usually stored in abandoned surface mine or dumped in landfills in the vicinity of the power plant. Previous studies have shown that toxic elements are leached from bottom ash and are transported to natural water sources (Binotto et al. 2000; Depoi et al. 2008; Levandowski and Kalkreuth 2009).

To provide the scientific community with initial order-of-magnitude nanominerals and nanoparticles emissions estimates from coal power plant, we report on new research concerning the physicochemical characterisation of coal and bottom ash (BA) nanoparticles produced within a Brazilian power plant, emphasising the importance of electron microscope investigation to the study of CDNs.

## Analytical procedures

Data provided by the Brazilian National Electricity Energy Agency (ANEEL 2006) show that approximately 11% of the electricity generated in Brazil is generated in seven coal-fed power plants in the states of Rio Grande do Sul, Santa Catarina and Paraná, which produce close to 1,500 MW of electric power. In the generation of electricity, these power plants produce approximately 3 Mt of ashes every year, which are composed from 65% to 85% of fly ash and 15% to 35% of bottom ash (Levandowski and Kalkreuth 2009). In addition, the existing coal-fired energy park in Brazil is planned to grow more than 2,000 MW with the entry into operation of five more power plants in Rio Grande do Sul State. When in full operation, this new scenario will raise the coal production to triple the current quantity, that is, almost 12 million tonnes/year (Rohde and Silva 2006).

Field work was performed during several weather seasons in 2008 (June and November), 2009 (February, April and December) and 2010 (January), including a comprehensive and detailed exploration of the study area around Santa Catarina power plant. A total of 21 coal and 21 bottom ash samples were collected in the principal Brazilian power plant (Santa Catarina State), which uses coal and generates approximately 850 MW/h of electricity. The incineration temperature in the combustion chamber is ca. 1,000–1,500°C. The feed coals before pulverisation and the associated bottom ash were simultaneously collected over a 5-day period. Samples containing about 15 to 20 kg of coal and ash were collected following ASTM (D 2234-89, 1991). In addition, coal samples from 12 coal mines in Santa Catarina State were collected and analysed to study local variations in chemical characteristics, with particular reference to any health risks and environmental concerns associated with coal use (Silva et al. 2009a).

The mineralogical composition of 21 coal and ash samples was determined by means of a Siemens model D5005 X-ray diffraction (XRD) and after XRD was selected seven samples for future analysis (chemical, petrology, SEM, TEM, Raman and others). Prior to the characterisation of coal and ash samples, it is important to know not only what kind of information a specific technique can provide (e.g. size distribution, elemental information, sensitivity, structural information etc.) but also the requirements of the sample (size range, elemental composition etc.) for each method to make analysis possible and to guarantee meaningful results (Tiede et al. 2009; Hower et al. 2008). Each technique has advantages and disadvantages, but only field emission scanning electron microscope (FE-SEM) and high-resolution transmission electron microscope (HR-TEM) currently allow the direct (real space) visualisation of nanoparticles. In this investigation, morphology, structure and composition of ultrafine minerals were investigated using a FE-SEM Zeiss Model ULTRA plus with charge compensation for all applications on conductive as well as non-conductive samples and a

200 keV JEOL-2010F HR-TEM equipped with an Oxford energy-dispersive X-ray detector and a scanning (STEM) unit (Silva et al. 2009a; Hower et al. 2008). The FE-SEM was equipped with an energy-dispersive X-ray spectrometer and the mineral identifications were made on the basis of morphology and grain composition using both secondary electron and back-scattered electron modes. Geometrical aberrations were measured by HR-TEM and controlled to provide less than a $\pi/4$ phase shift of the incoming electron wave over the probe-defining aperture of 14.5 mrad. The scanning acquisition was synchronised to the ac electrical power to minimise 60 Hz noise, and a pixel dwell time of 32 μs was chosen. EDS spectra were recorded in TEM image mode and then quantified using ES Vision software that uses the thin foil method to convert X-ray counts of each element into atomic or weight percentages. Electron diffraction patterns of the crystalline phases were recorded in SAED (selected area electron diffraction) or MBD (microbeam diffraction) mode, and the *d* spacings were compared to the International Center for Diffraction Data (ICDD 2009) inorganic compound powder diffraction file database to identify the crystalline phases.

Different suspensions, namely hexane, acetone, dichloromethane and methanol, were selected to prevent possible mineralogical changes in individual solvents. The suspension dissolves this "binder" material and breaks up aggregates to provide physically separated individual particles amenable for electron microscopes analysis. The suspension was pipetted onto lacycarbon films supported by Cu grids and left to evaporate before inserting the sample into the SEM and TEM. This method may have led to agglomeration but is a widely used standard procedure including metal sulphates (Giere et al. 2006). Before FE-SEM and STEM analysis, the TEM specimen holder was cleaned with a Gatan Model 950 Advanced Plasma System to minimise contamination. A drift correction system was used for the STEM–EDS mapping. Mineralogical analyses of the coal bottom ash subsamples were performed with ammonium oxalate and water in the absence of light: (1) 10 mg of CFA sample (five replicates) was mixed with ammonium oxalate reagent (28 g/L ammonium oxalate + 15 g/L oxalic acid solution, pH ~ 2.7). Samples were shaken in the dark for 4 h, then centrifuged (3,000 rpm, 10 min) and filtered (<22 μm). This extraction dissolves poorly crystalline Fe (III) oxides (e.g. ferrihydrite, schwertmannite) in the presence of more insoluble crystalline Fe (III) oxides (e.g. goethite, hematite) (Cornell and Schwertmann 2003; Peretyazhko et al. 2009). Sulphate-rich CDNs goethite of poor crystallinity can also be partially dissolved by acid ammonium oxalate; (2) 10 mg of CFA sample (five replicates) was mixed with water. Samples were shaken in the dark for 2 h, then centrifuged (3,000 rpm, 15 min) and filtered (<22 μm). This extraction dissolves gypsum, jarosite, alunogen, chalcanthite, hexahydrite, copiapite, epsomite, ferrohexahydrite, melanterite, rozenite and others minerals high solubles in water.

## Results and discussion

Brazilian coals have considerable concentrations of pyrite (Silva et al. 2009b), which has recently been shown to spontaneously generate hydrogen peroxide ($H_2O_2$) (Cohn et al. 2005) and hydroxyl radicals ($^{\bullet}OH$) (Cohn et al. 2004) when placed in water. The formation of these reactive oxygen species (ROS) also explains the recent observation that aqueous pyrite slurries degrade yeast RNA, ribosomal RNA and DNA (Cohn et al. 2006). Pyrite is thought to form $H_2O_2$ and is a strong oxidant (standard potential 1.80 and 0.87 V at pH 0 and 14, respectively) through the iron-catalysed Haber–Weiss reactions. Production of ROS such as the hydroxyl radical can then allow the transformation of amino acids and carbohydrates, initiate lipid peroxidation and oxidise nucleobases, thereby affecting human health (Kelly 2003; See et al. 2007). The hydroxyl radical is a strong oxidising agent capable of non-selectively oxidising a variety of organic compounds (e.g. Villa et al. 2008). In the Santa Catarina coals, the sulphides are typical authigenic nanominerals (Silva et al. 2010). Pyrite was the only Fe-containing nanomineral detected, changing gradually during combustion to form a Fe-containing glass and nanohematite. Figure 1 is a simple illustration of the pyrite nanocrystals in feed coal

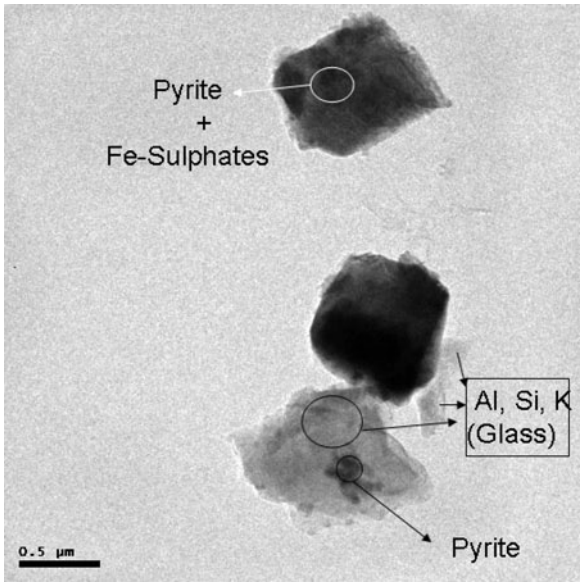


**Fig. 1** Pyrite and Al silicates glass in feed coals

mixed with silicate glass particles (e.g. Al–Si–K glass) and provides a clear illustration of the complexity of CDN chemistry in coal. In addition, the toxicity of elements in Brazilian coal, ashes and their environmental importance have been widely researched and documented (e.g. Depoi et al. 2008; Silva et al. 2009a, b). The potential toxicity and behaviour of nanoparticles in particular may be affected by a wide range of factors including particle atomic number and mass concentration, surface area, charge, chemistry and reactivity, size and size distribution, state of aggregation, elemental composition as well as structure and shape (Borm et al. 2006; Chau et al. 2007; Hochella et al. 2008).

The concentrations of As, Mo and Sb in Santa Catarina coals are lower than in coals from other Brazilian regions; Co, Hg, Pb, Mn, Li, Se, Be, Cd and Bi are within the range of Brazilian coals and are similar to the coal from Rio Grande do Sul State; concentrations of Cr, Cu, Ni, U, V and Zn are greater than for other Brazilian coals (Silva et al. 2009b). The HR-TEM study demonstrates the presence of nanoscale C deposits juxtaposed with and overgrown by slightly larger aluminosilicate (Al–Si) glassy spheres (Fig. 2), mullite, quartz, calcite, Fe oxides, Ca silicates, sulphates and other nanominerals (see Table 1). These nanocarbon agglomerates form an ultrathin halo or shell-like deposit on the coarser inorganic CDN. The spheres have aluminosilicate compositions with moderate abundance of Ca, Fe, K and Mg, and limited proportions of Na, Ti, S, P, Cl and trace elements. The C shells or nanocoatings are porous and consist of agglomerated nanometre-sized soot particles with characteristic concentric-onion ring structures. A majority of the Al–Si glassy spheres were found to have a C-based nanocoating or at least some fraction of the surface coated.

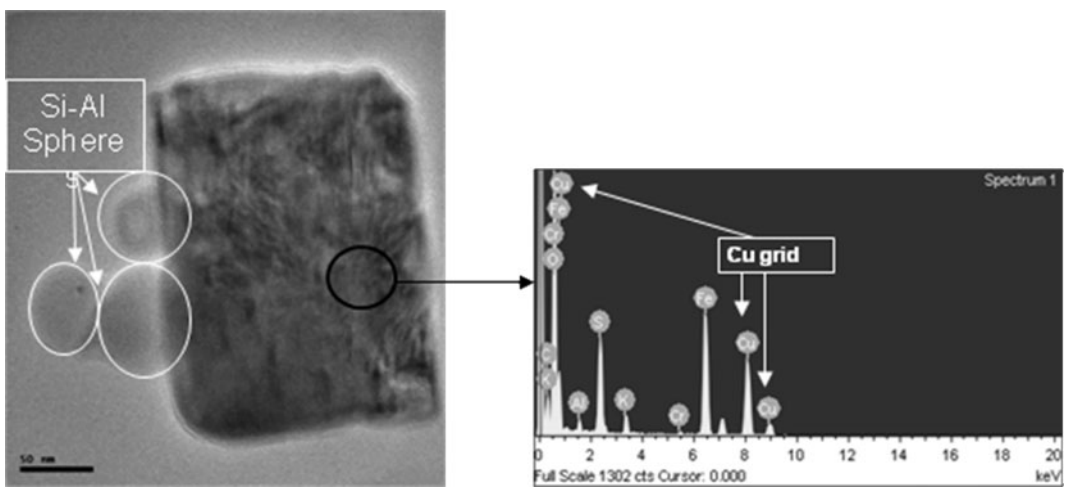


**Fig. 2** High-resolution transmission electron microscopy (HR-TEM) image of nanoclusters containing chromium

**Table 1** Nanominerals in coal and coal ashes identified by different analytical techniques

| Mineral name and formula | Coal | Bottom ash |
|---|---|---|
| Silicates | | |
| Actinolite, $Ca_2(Mg, Fe)_5Si_8O_{22}(OH)_2$ | a–b, d, f–g | b, f |
| Albite, $NaAlSiO_8$ | a, c–g | |
| Chamosite, $(Fe, Mg, Al)_6(Si, Al)_4O_{10}(O, OH)_8$ | a–g | a, c, g |
| Chlorite, $(Mg, Fe, Al)_6[(Si, Al)_4O_{10}][OH]_8$ | B | |
| Diopside, $CaMg(SiO_3)_2$ | | f–g |
| Hedenbergite, $CaFeSi_2O_6$ | a–c, g | |
| Illite, $[K_{0.75}(Al_{1.75}R^{2+}_{0.25})(Si_{3.50}Al_{0.50})O_{10}(OH)_2$ (R = Fe, Mg, Ti] | b–g | a–f |
| Kaolinite, $Al_2Si_2O_5(OH)_4$ | c–g | a–g |
| Microcline, $KAlSi_3O_8$ | a–g | f |
| Quartz, $SiO_2$ | a–g | a–g |
| Zircon, $ZrSiO_4$ | b, d–g | |
| Sulphides | | |
| Galena, PbS | a–g | |
| Pyrite, $FeS_2$ | a–g | |
| Marcasite, $FeS_2$ | b–d, f | |
| Pyrrhotite $Fe_{(1-x)}S$ | a–c, f–g | f–g |
| Chalcopyrite, $CuFeS_2$ | a, d, f–g | |
| Sphalerite, ZnS | a–g | |
| Carbonates | | |
| Ankerite, $(Fe,Ca,Mg)CO_3$ | a–f | a–c, f–g |
| Calcite, $CaCO_3$ | a–g | |
| Dolomite, $CaMg(CO_3)_2$ | d, f | |
| Siderite, $FeCO_3$ | a–f | |
| Oligonite, $Fe(Mn, Zn)(CO_3)$ | c–f | |
| Phosphates | | |
| Brushite, $CaPO_3(OH) \cdot 2H_2O$ | b, d–g | |
| Monazite, $(Ce, La, Th, Nd, Y)PO_4$ | a–g | |
| Sulphates | | |
| Anhydrite, $CaSO_4$ | b, d–f | g |
| Alunogen, $Al_2(SO_4)_3 \cdot 17H_2O$ | g | |
| Barite, $BaSO_4$ | a–g | |
| Calcantite, $CuSO_4 \cdot 5H_2O$ | c | |
| Epsomite, $MgSO_4 \cdot 7H_2O$ | c–f | |
| Ferrohexahydrite, $FeSO_4 \cdot 6H_2O$ | c | |
| Hexahydrite, $MgSO_4 \cdot 6H_2O$ | b–g | b–g |
| Gypsum, $Ca[SO_4] \cdot 2H_2O$ | a–g | a–g |
| Jarosite, $KFe^{3+}_3(SO_4)_2(OH)_6$ | b–g | a–g |
| Melanterite $FeSO_4 \cdot 7H_2O$ | c–g | f |
| Natrojarosite, $NaFe_3(SO_4)_2(OH)_6$ | a–g | |
| Rozenite, $FeSO_4 \cdot 4H_2O$ | c, e | |
| Sideronatrite, $Na_2Fe[SO_4](OH) \cdot 3H_2O$ | b–d, f | |
| Schwertmannite, $Fe^{3+}_{16}O_{16}(OH)_{12}(SO_4)_2$ | a–f | c, f–g |
| Szomolnokite, $FeSO_4 \cdot H_2O$ | b | |
| Oxides and hydroxides | | |
| Anthophylite, $(Mg,Fe^{2+})_7Si_8O_{22}(OH)_2$ | | f |
| Delafossite, $CuFeO_2(Cu_2O \cdot Fe_2O_3)$ | | f–g |
| Brownmillerite, $Ca_4Al_2Fe_2O_{10}$ | | |
| Calcium iron aluminium oxide, $CaAl_2Fe_4O_{19}$ | b–e | |
| Chromite $FeCr_2O_4$ | | a, c, f |
| Goethite, $Fe(OH)_3$ | a–f | f |
| Hematite, $\alpha$-$Fe_2O_3$ | c–g | a–g |

**Table 1** (continued)

| Mineral name and formula | Coal | Bottom ash |
|---|---|---|
| Hercynite, $FeAl_2O_4$ | a–g | |
| Maghemite $\gamma$-$Fe_2O_3$ | b, f | a–g |
| Magnesioferrite, $MgFe_2O_4$ | b–f | |
| Magnetite, $Fe_3O_4$ | | a–g |
| Rutile, $TiO_2$ | a–g | b, d–g |
| Wuestite, FeO | b, c | |
| Others | | |
| Arrojadite, $Na_2(Fe, Mn)_5(PO_4)_4$ | b | f |
| Calcium ferrite, $CaFe_2O_4$ | e | |
| Columbite, $(Fe, Mn)Nb_2O_6$ | b, c, f | |
| Ilmenite, $FeTiO_3$ | a–c, f | |
| Magnesioferrite, $MgFe_2O_4$ | a–b, d–f | |

(a) power plant sample 10, (b) power plant sample 11, (c) power plant sample 12, (d) power plant sample 13, (e) power plant sample 14, (f) power plant sample 15, (g) power plant sample 16

The nanooxides detected in bottom ash include anatase, brownmillerite, chromite, columbite, delafossite, hematite, hercynite, ilmenite, maghemite magnesioferrite, magnetite, quartz, rutile and wuestite. Some of these phases may be products of oxidation of pyrite and reactions with calcite. In addition, Fe oxides (mainly hematite and magnetite) are the main bottom ash products of the oxidation of pyrite. Whereas some of our nanohematite (e.g. Fig. 3a) suggest direct transformation of pyrite upon heating in air, others show transformation into hematite via an intermediate stage involving pyrrhotite growth (Bhargava et al. 2009; Bunt and Waanders 2009; Bunt et al. 2008; Jorgensen and Moyle 1982; Schorr and Everhart 1969).

The hazard for human health caused by occupational exposure to airborne inorganic particles, such as quartz, silica and some sheet silicates, is definitively established (Belluso et al. 2006) with a grain size of less than 10 μm (PM10) thought to pose a considerably greater health hazard, and this health risk may increase as the grain size becomes smaller (Balaan and Banks 1998). In addition, an alternative contributing factor identified via recent ecological analysis (Tian 2005) is that concentrations of coal-derived BA ultrafine and nanoparticulate (<50 nm, e.g. Fig. 4a) crystalline silica correlate with the incidence of lung cancer (Tian 2005), and in 1997 the World Health Organization's International Agency for Research on Cancer reclassified quartz and crystalline silica from a class 2 (1987 evaluation) carcinogen to a class 1 carcinogen, stating that sufficient evidence existed for carcinogenicity of quartz in both humans and experimental animals. This creates the fascinating prospect that the environmental conditions that resulted in the extinction event may have produced particularly toxic coal and bottom ash chemistry that is affecting the people using it today. Globally, although coal is sometimes closely associated with the boundary, no other examples of its widespread domestic utilisation are known to us. Quartz was dominantly fine-grained and abundant in evaluated bottom ashes (e.g. Fig. 4a). Only a small proportion of quartz appears to be detrital. We have proposed an effective technique to identify nanoquartz particles in coal BA by HR-TEM/EDS because the potential ecotoxicity of these nanoquartz (e.g. Fig. 4a) is already of considerable interest (Warheit et al. 2007, 2009), and given in the coal bottom ash they represent an as yet unevaluated additional health risk to power plant emissions.

One other class of nanominerals—the Fe oxides—has arguably provided the main focus for environmental nanoparticle research (Waychunas et al. 2005a, b), and a large number of authors have examined the adsorption of arsenic and chromium by iron oxides (see reviews by Smedley and Kinniburgh 2002; Mohan and Pittman 2007; Silva et al. 2009a), highlighting (a) the tendency of As (in both of its common $As^{3+}$ and $As^{5+}$ states) and Cr (in both of its common $Cr^{6+}$ state) to strongly bind to (hydrous) Fe oxides (as monodentate or bidentate inner sphere complexes), even at very low arsenic concentrations, and (b) the important environmental role of amorphous,

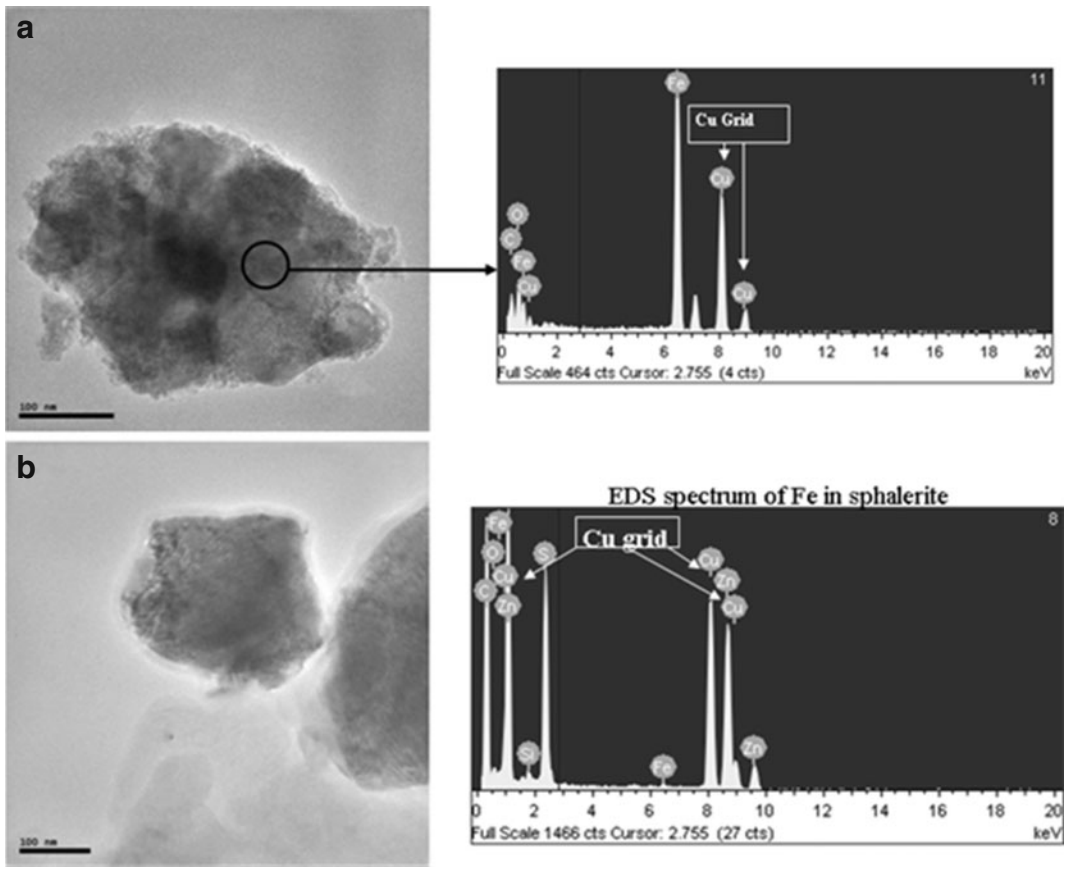


**Fig. 3** HR-TEM image and EDS spectrum: **a** showing the very fine ordered hematite structures nanoparticles and **b** sphalerite in feed coals

freshly precipitated Fe oxides as sorbents of arsenic and chromium. Brown et al. (1998) note the successful in situ application of an acidified solution of ferrous sulphate heptahydrate (via a combination of wells and trenches) to remove Cr (VI). Mohan and Pittman (2007) reviewed the

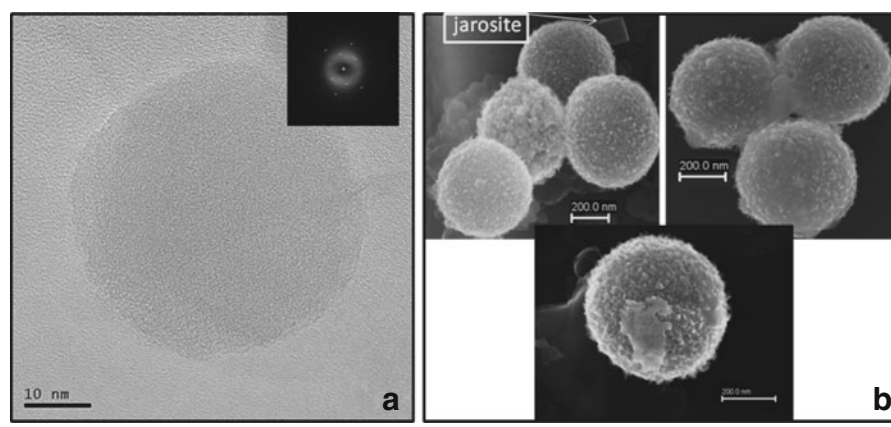


**Fig. 4** **a** HR-TEM and Fourier transformation (FFT) confirm the size of nanoquartz sphere; **b** FE-SEM of submicronic spheres, containing Zr, Ni, Mg and Al

performance of the main arsenic-removal technologies, including those utilising iron as an adsorbent or precipitant.

Inorganic nanoparticles are a distinct class of matter because their properties can be substantially modified relative to the bulk material. In addition, nanoscale minerals, such as hematite ($\alpha$-$Fe_2O_3$), are extremely common natural products of biomineralisation (Fowler et al. 1999) and chemical weathering reactions (Gilbert and Banfield 2005). Although frequently a minority fraction, mineral nanoparticles can have a profound impact on their environment (Gilbert and Banfield 2005), having high surface areas and hence high reactivity and total energy relative to macroscopic minerals. Hematite, like the other iron oxide minerals, is of particular interest because its properties at different sizes indicate a wide range of geochemical reactivity (Madden et al. 2006). This includes adsorption of ions from solution, such as phosphates (Waychunas et al. 2005a) and arsenates (Waychunas et al. 2005b), photochemical reduction in aqueous solution (Sherman 2005) and heterogeneous catalysis (Feng et al. 2004). Atomistic simulations have been used to describe the structure, stability and properties of bulk minerals (Cooke et al. 2004), mineral surfaces (Kerisit and Parker 2004) and discrete nanoparticles (Feng et al. 2006). The structures and stabilities of single nanoparticles have been calculated and it has been demonstrated that these are dependent upon environmental conditions (Zhang and Banfield 2004). Many experimental and theoretical studies have considered the interactions between nanoparticles and different types of surface ligands. According to results from Zhang et al. (2007), the following is inferred. First, nanoparticles can accommodate more adsorbates per unit surface area than the corresponding bulk material because the surfaces of the former are more structurally open for coordination of absorbates. Second, adsorbates may bind with nanoparticles more strongly than with the corresponding bulk material because the binding energy for the former is higher than for the latter. These factors may be important for assessment of the environmental roles and impact of nanoparticles from coal and bottom ashes.

In the studied bottom ashes with regard to Al-, Zr-, Ni- and Mg-bearing particles, these are typically sub-micronic spherical and show a size range of 250–350 nm (see Fig. 4b). The chemical composition and morphology of 36 sub-micronic spheres studied in the BA (e.g. Fig. 4b) reveal the common presence of abundant aluminosilicate glass, ferrian spinel, hematite; magnetite, mullite and quartz. The chemical composition of these spheres is extremely variable, this being a likely consequence of the high-temperature/low-pressure metamorphic reactions created by the coal combustion process. Within the studied Brazilian feed coals burnt at this power station, Zr is initially present predominantly as the accessory mineral zircon ($ZrSiO_4$), whereas Ni is mostly associated with sulphides such as millerite (NiS). Upon combustion, however, these elements become redistributed within secondary high-temperature minerals, notably in aluminosilicates such as mullite as well as aluminosilicate glass.

The nanominerals from coal bottom ashes (BA) and their thermodynamic stability diagrams will be discussed in a future paper that will also include studying the thermodynamics and by-products of coal combustion, estimating emissions associated with different coal ranks and examining the potential environmental and health impacts on residential communities near the coal power plants. Clearly, nanominerals and nanoparticles from feed coal and bottom ashes are a topic of expanding scientific interest, and significant research is required to fill current knowledge gaps.

## Overview and conclusions

The pulmonary toxicity of airborne particles has been well studied, and it is known that toxicity is strongly related to particle size (Frampton et al. 2006; Geiser et al. 2005; Brown et al. 2001) and the presence of transition metals such as iron (Smith et al. 2007; Pritchard et al. 1996). Iron is the most abundant transition metal in ambient particulate especially around the Santa Catarina power plant. However, although some studies suggest ecotoxicity, the detailed toxicity of bottom ash

nanoparticles and their effects on human health, as well as their environmental fate and impact in water and soil, is still largely unknown. It has been reported that different types of nanoparticles can cause cytotoxicity and cross cellular layers (Koch et al. 2005; Hardman 2006) or can accumulate in tissue (Bullard-Dillard et al. 1996). In addition, data clearly show that the population living in at least one investigated area (Santa Catarina, Brazil) has been exposed to an increased environmental risk due to a coal-fired power plant. This suggests that longer-term monitoring is needed around coal power plants to better quantify emissions of individual power plants in the world.

The combination of FE-SEM and HR-TEM/EDS as used in this study provides a powerful technique to characterise nanoparticles for environmental studies. Our study further demonstrates the complexity of mineralogical relationships between nanominerals present in coals and bottom ashes produced during coal combustion, yielding observations impossible to make using more traditional characterisation methods such as optical petrography. Our results suggest that the volatility of chemical forms of trace metals in raw coal and the chemical change of trace metals during high-temperature heat processing have not been sufficiently addressed. Our approach is an important step toward a realistic description of nanoparticle structure that includes internal strain, which is likely to be a general feature of nanoscale solids present in coal and bottom ash.

Furthermore, given what is already known about the health effects of airborne particulate matter in general, and nanoparticles in particular, it is likely that the population living close to power plants such as Santa Catarina are being subjected to greater health risks linked to CDNs inhalation. Studies on bottom ash nanoparticles, such as the data presented here, emphasise the need for detailed epidemiological investigation of disease patterns around industrial CDN point sources.

**Acknowledgements** The authors express their gratitude to the heartfelt help of FEHIDRO, Environmental Foundation of Santa Catarina State—FATMA and Ferrovia Teresa Cristina. The manuscript was much improved by the comments of Drs. Xavier Querol and Teresa Moreno. Thanks are also expressed to Tractebel Energia—SUEZ, especially Jose L. Magri, for providing other data relevant to the study and for assistance in collecting the samples. The research for this study was carried out with support from the IPADHC for coal in sustainable development, funded in part by the IPADHC and FEHIDRO government of Santa Catarina State, Brazil. This work was financially supported by the FEHIDRO. We acknowledge Dr. F. Macias for the assistance with FE-SEM and HR-TEM analysis.

## References

An, D., Li, D., Liang, Y., & Jing, Z. (2007). Unventilated indoor coal-fired stoves in Guizhou province, China: Reduction of arsenic exposure through behavior changes resulting from mitigation and health education in populations with arsenicosis. *Environmental Health Perspectives, 115*, 659–662.

ANEEL (2006). Agência Nacional de Energia Elétrica. http://www.aneel.gov.br. Accessed 25 June.

ASTM (1991). Annual Book of ASTM Standards. Sec 05.05. Standard test method for ash in the analysis sample of coal and coke from coal, Philadelphia, PA.

Balaan, M. R., & Banks, D. E. (1998). Chapter 29: Silicosis. In W. N. Rom (Ed.), *Environmental and occupational medicine* (3rd ed.). New York: Lippincott-Raven.

Belluso, E., Bellis, D., Fornero, E., Capella, S., Ferraris, G., & Coverlizza, S. (2006). Assessment of inorganic fibre burden in biological samples by scanning electron microscopy–energy dispersive spectroscopy. *Microchimica Acta, 155*, 95.

Bhargava, S., Garg, A., & Subasinghe, N. (2009). In situ high-temperature phase transformation studies on pyrite. *Fuel, 88*, 988–993.

Binotto, R. B., Teixeira, E. C., Sanchez, J. C. D., Migliavacca, D., & Nani, A. S. (2000). Environmental assessment: contamination of phreatic aquifer in areas impacted by waste from coal processing activities. *Fuel, 79*, 1547–1560.

Borm, P., Robbins, D., & Haubold, S. (2006). The potential risks of nanomaterials: A review carried out for ECETOC. *Particle and Fibre Toxicology, 3*, 11. doi:10.1186/1743-8977-3-11.

Brown, D., Wilson, M., MacNee, W., Stone, V., & Donaldson, K. (2001). Size-dependent proinflammatory effects of ultrafine polystyrene particles: A role for surface area and oxidative stress in the enhanced activity of ultrafines. *Toxicology and Applied Pharmacology, 175*, 191–199.

Brown, R. A., Leahy, M. C., & Pyrih, R. Z. (1998). In situ remediation of metals comes of age. *Remediation, 8*, 81–96.

Bullard-Dillard, R., Creek, K., Scrivens, W., & Tour, J. (1996). Tissue sites of uptake of C-14-labeled C-60. *Bioorganic Chemistry, 24*, 376–385.

Bunt, J., & Waanders, F. (2009). Pipe reactor gasification studies of a South African bituminous coal blend. Part

1—carbon and volatile matter behaviour as function of feed coal particle size reduction. *Fuel, 88*, 585–594.

Bunt, J., Joubert, J., & Waanders, F. (2008). Coal char temperature profile estimation using optical reflectance for a commercial-scale Sasol–Lurgi FBDB gasifier. *Fuel, 87*, 2849–2855.

Chau, C., Wu, S., & Yen, G. (2007). The development of regulations for food nanotechnology. *Trends in Food Science & Technology, 18*, 269–280.

Chen, Y., Shah, N., & Huggins, F. (2005). Characterization of ultrafine coal fly ash particles by energy-filtered TEM. *Journal of Microscopy, 217*, 225–234.

Chen, Y., Shah, N., Huggins, F. E., & Huffman, G. P. (2004). Investigation of the microcharacteristics of PM2.5 in residual oil fly ash by analytical transmission electron microscopy. *Environmental Science and Technology, 38*, 6553–6560.

Cohn, C., Borda, M., & Schoonen, M. (2004). RNA decomposition by pyrite-induced radicals and possible role of lipids during the emergence of life. *Earth and Planetary Science Letters, 225*, 271–278.

Cohn, C., Mueller, S., Wimmer, E., Leifer, N., Greenbaum, S., Strongin, D. R., et al. (2006). Pyrite-induced hydroxyl radical formation and its effect on nucleic acids. *Geochemical Transactions, 7*, 3.

Cohn, C., Pak, A., Schoonen, M., & Strongin, D. (2005). Quantifying hydrogen peroxide in iron-containing solutions using leuco crystal violet. *Geochemical Transactions, 6*, 47–52.

Cooke, D. J., Redfern, S. E., & Parker, S. C. (2004). Atomistic simulation of the structure and segregation to the (0001) and surfaces of $Fe_2O_3$. *Physics and Chemistry of Minerals, 31*, 507–517.

Cornell, R. M., & Schwertmann, U. (2003). *The iron oxides: Structure, properties, reactions, occurrence and uses, second, completely revised and extended ed*. Weinheim: Wiley-VCH.

Depoi, F. S., Pozebon, D., & Kalkreuth, W. D. (2008). Chemical characterization of feed coals and combustion-by-products from Brazilian power plants. *International Journal of Coal Geology, 76*, 227–236.

Effros, R. (2009). The canary in the coal mine: Telomeres and human healthspan. *Journals of Gerontology, Series A: Biological Sciences and Medical Sciences, 64*, 511–515.

Feng, J. Y., Hu, X. J., & Yue, P. L. (2004). Discoloration and mineralization of orange II using different heterogeneous catalysts containing Fe: A comparative study. *Environmental Science & Technology, 38*, 5773–5778.

Feng, X. S., Dean, C., Zhong, L., Paras, M. S., Santora, B., Sutorik, A. C., et al. (2006). Converting ceria polyhedral nanoparticles into single-crystal nanospheres. *Science, 312*, 1504–1508.

Fowler, T. A., Holmes, P. R., & Crundwell, F. K. (1999). Mechanism of pyrite dissolution in the presence of *Thiobacillus ferrooxidans*. *Applied and Environmental Microbiology, 65*, 2987–2993.

Frampton, M., Stewart, J., Oberdorster, G., Morrow, P., Chalupa, D., Pietropaoli, A., et al. (2006). Inhalation of ultrafine particles alters blood leukocyte expression of adhesion molecules in humans. *Environmental Health Perspectives, 114*, 51–58.

Geiser, M., Rothen-Rutishauser, B., Kapp, N., Schurch, S., Kreyling, W., Schulz, H., et al. (2005). Ultrafine particles cross cellular membranes by nonphagocytic mechanisms in lungs and in cultured cells. *Environmental Health Perspectives, 113*, 1555–1560.

Giere, R., Blackford, M., & Smith, K. (2006). TEM study of PM2.5 emitted from coal and tire combustion in a thermal power station. *Environmental Science & Technology, 40*, 6235–6240.

Gilbert, B., & Banfield, J. F. (2005). Molecular-scale processes involving nanoparticulate minerals in biogeochemical systems. *Reviews in Mineralogy and Geochemistry, 59*, 109–155.

Gilmour, M., O'Connor, S., Dick, C., Miller, C., & Linak, W. (2004). Differential pulmonary inflammation and in vitro cytotoxicity of size-fractionated fly ash particles from pulverized coal combustion. *Journal of the Air & Waste Management Association, 54*, 286–295.

Hardman, R. (2006). A toxicologic review of quantum dots: Toxicity depends on physicochemical and environmental factors. *Environmental Health Perspectives, 114*, 165–172.

Hochella, M., Lower, S., Maurice, P., Penn, L., Sahai, N., Sparks, D., et al. (2008). Nanominerals, mineral nanoparticles, and earth systems. *Science, 319*, 1631–1635.

Hower, J., Graham, U., Dozier, A., Tseng, M., & Khatri, R. (2008). Association of the sites of heavy metals with nanoscale carbon in a Kentucky electrostatic precipitator fly ash. *Environmental Science & Technology, 42*, 8471–8477.

ICDD, International Center for Diffraction Data (2009). http://www.icdd.com. Accessed 20 July 2009.

Jorgensen, F., & Moyle, F. (1982). Phases formed during the thermal analysis of pyrite in air. *Journal of Thermal Analysis, 25*, 473–485.

Kelly, F. (2003). Oxidative stress: Its role in air pollution and adverse health effects. *Occupational and Environmental Medicine, 60*, 612–616.

Kerisit, S., & Parker, S. C. (2004). Free energy of adsorption of water and metal ions on the {10.hivin.14} calcite surface. *Journal of the American Chemical Society, 126*, 10152–10161.

Koch, A., Reynolds, F., Merkle, H., Weissleder, R., & Josephson, L. (2005). Transport of surface-modified nanoparticles through cell monolayers. *ChemBioChem, 6*, 337–345.

Levandowski, J., & Kalkreuth, W. (2009). Chemical and petrographical characterization of feed coal, fly ash and bottom ash from the Figueira Power Plant, Paraná, Brazil. *International Journal of Coal Geology, 77*, 269–281

Liang-Che, C., Jo-Chi, T., & Chung-Ching, H. (2006). Gene polymorphisms of fibrinolytic enzymes in coal workers pneumoconiosis. *Archives of Environmental & Occupational Health, 61*, 61–66.

Madden, A. S., Hochella, M. F., & Luxton, T. P. (2006). Insights for size-dependent reactivity of hematite nanomineral surfaces through $Cu^{2+}$ sorp-

tion. *Geochimica et Cosmochimica Acta, 70*, 4095–4104.
Mohan, D., Pittman, C. U. Jr. (2007). Arsenic removal from water/wastewater using adsorbents—a critical review. *Journal of Hazardous Materials, 142*, 1–53.
Oberdoerster, G., Oberdoerster, E., & Oberdoerster, J. (2005). Nanotoxicology: An emerging discipline evolving studies of ultrafine particles. *Environmental Health Perspectives, 113*, 823–839.
Peretyazhko, T., Zachara, J. M., Boily, J. F., Xia, Y., Gassman, P. L., Arey, B. W., et al. (2009). Mineralogical transformations controlling acid mine drainage chemistry. *Chemical Geology, 262*, 169–178.
Pritchard, R., Ghio, A., Lehmann, J., Winsett, D., Tepper, J., Park, P., et al. (1996). Oxidant generation and lung injury after particulate air pollutant exposure increase with concentrations of associated metals. *Inhalation Toxicology, 8*, 457–477.
Rastogi, N., Oakes, M., Schauer, J., Shafer, M., Majestic, B., & Weber, R. (2009). New technique for online measurement of water-soluble Fe(II) in atmospheric aerosols. *Environmental Science & Technology, 43*, 2425–2430.
Rohde, G. M., & Silva, N. I. W. (2006). *Cinzas de Carvão Fóssil no Brasil Aspectos Técnicos e Ambientais* (Vol. 1). Porto Alegre: CIENTEC.
Schorr, J., & Everhart, J. (1969). Thermal behavior of pyrite and its relation to carbon and sulfur oxidation in clays. *Journal of the American Ceramic Society, 52*, 351–354.
See, S., Wang, Y., & Balasubramanian, R. (2007). Contrasting reactive oxygen species and transition metal concentrations in combustion aerosols. *Environmental Research, 103*, 317–324.
Sherman, D. M. (2005). Electronic structures of iron(III) and manganese(IV) (hydr)oxide minerals: Thermodynamics of photochemical reductive dissolution in aquatic environments. *Geochimica et Cosmochimica Acta, 69*, 3249–3255.
Silva, L. F. O., Macias, F., Oliveira, M. L. S., da Boit, K. M., & Waanders, F. (2010). Coal cleaning residues and Fe-minerals implications. *Environmental Monitoring and Assessment*. doi:10.1007/s10661-010-1340-8.
Silva, L. F. O., Moreno, T., & Querol, X. (2009a). An introductory TEM study of Fe-nanominerals within coal fly ash. *Science of the Total Environment, 407*, 4972–4974.
Silva, L. F. O., Oliveira, M. L. S., da Boit, K. M., & Finkelman, R. B. (2009b). Characterization of Santa Catarina (Brazil) coal with respect to Human Health and Environmental Concerns. *Environmental Geochemistry and Health, 31*, 475–485.
Smedley, P. L., & Kinniburgh, D. G. (2002). A review of the source, behaviour and distribution of arsenic in natural waters. *Applied Geochemistry, 17*, 517–68.
Smith, C., Shaw, B., & Handy, R. (2007). Toxicity of single walled carbon nanotubes to rainbow trout (*Oncorhynchus mykiss*): respiratory toxicity, organ pathologies, and other physiological effects. *Aquatic Toxicology, 82*, 94–109.
Suzuki, Y., Kelly, S., Kemner, K., & Banfield, J. (2002). Radionuclide contamination—nanometre-size products of uranium bioreduction. *Nature, 419*, 134–134.
Tatár, E., Csiky, G., Mihucz, V., & Záray, G. (2005). Investigation of adverse health effects of residual oil fly ash emitted from a heavy-oil-fuelled Hungarian power plant. *Microchemical Journal, 79*, 263–269.
Tian, L. (2005). *Coal combustion emissions and lung cancer in Xuan Wei, China*. PhD thesis, University of California: Berkeley, CA, 2005.
Tiede, K., Hassellöv, M., Breitbarthc, E., Chaudhryb, Q., & Boxall, A. B. A. (2009). Considerations for environmental fate and ecotoxicity testing to support environmental risk assessments for engineered nanoparticles. *Journal of Chromatography A, 1216*, 503–509.
Villa, R. D., Trovo, A. G., & Pupo, N. R. F. (2008). Environmental implications of soil remediation using the Fenton process. *Chemosphere, 71*, 43–50.
Warheit, D. B., Webb, T. R., & Reed, K. L. (2007). Pulmonary toxicity screening studies in male rats with M5 respirable fibers and particulates. *Inhalation Toxicology, 19*, 951.
Warheit, D. B., Reed, K. L., Sayes, C. M. (2009). A role for nanoparticle surface reactivity in facilitating pulmonary toxicity and development of a base set of hazard assays as a component of nanoparticle risk management. *Inhalation Toxicology, 21*, 61.
Waychunas, G., Kim, C., & Banfield, J. (2005a). Nanoparticulate iron oxide minerals in soils and sediments: Unique properties and contaminant scavenging mechanisms. *Journal of Nanoparticle Research, 7*, 409–433.
Waychunas, G., Trainor, T., Eng, P., Catalano, J., Brown, G., Davis, J., et al. (2005b). Surface complexation studied via combined grazing-incidence EXAFS and surface diffraction: Arsenate and hematite (0 0 0 1) and (1 0–1 2). *Analytical and Bioanalytical Chemistry, 383*, 12–27.
Xia, T., Lovochick, M., & Brant, J. (2006). Comparisons of the ability of ambient and manufactured nanoparticles to induce cellular toxicity according to an oxidative stress paradigm. *Nano Letters, 6*, 1794–1897.
Zhang, H., & Banfield, J. F. (2004). Aggregation, coarsening, and phase transformation in ZnS nanoparticles studied by molecular dynamics simulations. *Nano Letters, 4*, 713–718.
Zhang, H., Rustad, J. R., & Banfield, J. F. (2007). Interaction between water molecules and zinc sulfide nanoparticles studied by temperature-programmed desorption and molecular dynamics simulations. *Journal of Physical Chemistry A, 111*, 5008–5014.